

ORIGINAL ARTICLE

Study on Die Shoulder Patterning Method (DSPM) to Minimise Springback of U-Bending

N.J. Baharuddin, A.R. Abdul Manaf and A.S. Jamaludin

Faculty of Manufacturing Engineering, Universiti Malaysia Pahang, 26600 Pahang, Malaysia.

ABSTRACT – U-bending is increasingly used in the sheet metal industry such as car door pillars. However, springback phenomenon always tends to occur after removing sheet metal from the fixtures and resulting in changing product effectiveness, wasting material as well as increasing manufacturing costs. Thus, minimizing springback in the bending of sheet metal is vital to maintain close geometric tolerances in the deformed part. Many researchers have done investigated and predicted the springback occurrence by experiments and simulations. Nevertheless, there is no actual study on the die shoulder patterning method (DSPM) to reduce springback of hat-shaped parts. In this paper, the hat-shaped part is deformed using the new developed forming method and have been experimented with as well as validated using three-way Anova and graphical analysis. As expected, DSPM dominates the springback sensitivity, with higher contact area reducing the springback of hat-shaped parts. For AISI 1030 of pattern 2, springback is dramatically reduced as the sliding stress between the die shoulder and surface of the blank is optimized.

ARTICLE HISTORY

Received: 23rd Mar 2021

Revised: 7th Feb 2022

Accepted: 10th Mar 2022

KEYWORDS

U-bending;

Springback;

DSPM;

Surface engineering;

Optimization

INTRODUCTION

U-bending of sheet metal has been increasingly used in the manufacture of beams and car fenders [1-2]. Most manufacturers agree that this forming process is the easiest and most useful method in forming the hat-shaped parts of the metal. It also facilitates mass production as it has the potential to manufacture the same item at a remarkably high pace at low costs and with outstanding quality. The U-bending process involves three main steps, namely bending, forming, and unloading as shown in Figure 1. Generally, the deformation of the metal using the U-bending mechanism involves the force of a punch to the blank with constant speed and pressure in the downward direction according to the dimension of the die. However, the springback phenomenon has become a growing concern for manufacturers as they rely on various sheet metals such as low-carbon steel and advanced high—strength steel (AHSS). Sheet metal in low carbon steel is likely to return to its original form after its removal from the fixture grips. The springback phenomenon is described as the elastically-driven changes in the shape of a part upon unloading after the forming process. Hence, the occurrence of springback tends to appear after bending the parts, thus affecting product accuracy, increasing rejection as well as manufacturing costs.

Springback reduction is necessary during the die design to obtain definite final shapes. Numerous techniques have been performed by manufacturers and researchers to minimise springback correction during the forming process. For example, numerical predictions based on fundamental theories or assumptions of engineering beams in U-bending were developed in previous studies on springback behaviour [3–5]. The authors modified the tool curves for bending the sheet metal under minimal tension. However, these assumptions can only be implemented for a small springback in pure bending cases [6]. A previous study was performed using controlled experiments of springback under practical forming conditions (i.e. involving bending and unloading simultaneously with applied friction and sliding over the tooling) [7]. Other researchers focused on material indirect realistic experiments such as stretch-bend tests or tensile tests and showed that these tests were not suited for final parts in large scale production.

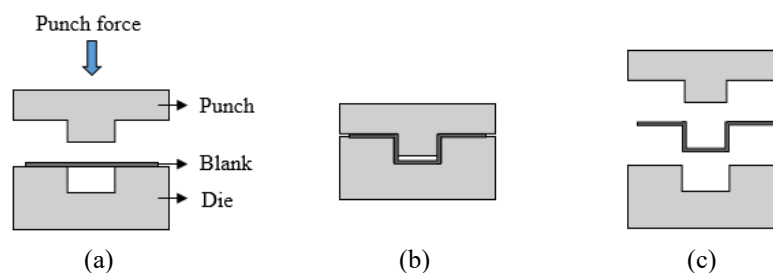


Figure 1. Schematic diagram of the U-bending, (a) setup, (b) bending, and (c) unloading process.

In this study, a new method of springback correction was performed using a set of inserts that was patterned on the corner shoulder to produce the best final hat-shaped parts in the U-bending process. Specifically, the U-bending process was performed utilising the hydraulic pressing machine as it is commonly used in the manufacture of hat-shaped parts. The machine includes a press holding time in seconds for a pre-set period of time which acts as one of the bending condition parameters [8–10]. The forming process of U-bending requires several critical parameters for sheet metal to bend into the desired shape with the assistance of a pair of tools known as the punch and die that is attached to the body of the hydraulic press machine.

DIE SHOULDER PATTERNING METHOD (DSPM)

A novel die surface patterning method (DSPM) to improve the structural integrity of hat-shaped components is introduced in this study. Over the years, surface patterning has been widely recognised for its crucial role in the structural integrity of engineering components [11-12]. Godi previously designed a new typology of patterned surfaces using the axial sliding technique (AST) that successfully reduced up to half of the frictional forces at normal loads compared to unpatterned surfaces. The authors stated that it improved the components' performance such as carrying a systematic load and offering extra-lubrication valleys [13]. However, their micro-patterned AST was only suitable for rod-type components and not applicable to hat-shaped components.

For most of the forming processes, the tool shoulder has a significant relationship with the springback radius and acts as friction in the formation of the components into the desired shape. Four different types of DSPM were designed in this study as shown in Table 1. A set of DSPM without the treatment of a 5mm radius pattern was used as the standard and designed without using DSPM to differentiate between DSPM and non-DSPM. Three sets of patterns were differentiated by pattern, rib size, and pitch distance as shown in Figure 2. For each experiment, a set of patterns was clamped inside the body of the dies and three specimens with different blank widths, *b*, were formed into the hat-shaped part. The hat-shaped part was deformed by the standard U-bending method. The U-bending process was conducted using a hydraulic press machine, and the parameters were selected based on previous studies and availability. Next, the measurement analysis of the formed hat-shaped parts was investigated using a coordinate measuring machine (CMM) to reveal the nature of the springback after removal from the fixture’s grips.

Table 1. Design of die shoulder patterning.

No.	Pattern	Type	Radius corner, R_d (mm)	Rib size, d_o (mm)	Pitch distance, d_p (mm)
i.	No pattern, P_0	Non-vertical	5	0	0
ii.	Pattern 1, P_1	Vertical	5	2	0.2
iii.	Pattern 2, P_2	Vertical	5	2	0.4
iv.	Pattern 3, P_3	Vertical	5	2	1

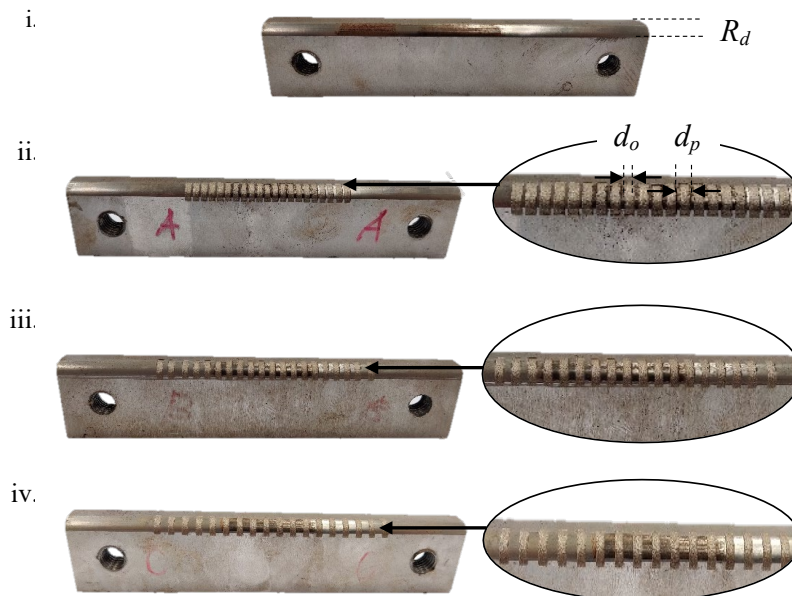


Figure 2. The inserts of die surface patterning method.

EXPERIMENT PROCEDURES

U-Bending

The experiment used DSPM based on a previous study on roll bending [14]. The U-bending process was operated using a hydraulic press machine with selected bending conditions. For the U-bending test operated using this machine, it

was necessary to set up the newly designed U-bending jig to the machine. Test conditions were established according to the available parameters of the machine as shown in Table 2 where the press holding time (p_t) values were selected as 1, 3, and 5 seconds. The punch force (F_p) and punch speed (S_p) were kept constant throughout the test as these conditions cannot be controlled by the machine. Besides, the three different blank widths of 20 mm, 25 mm, and 30 mm acted as variable parameters. The thickness and length of the blank were kept as constant parameters, while the internal bend radius or punch radius and external bend radius or die radius are shown in Figure 3.

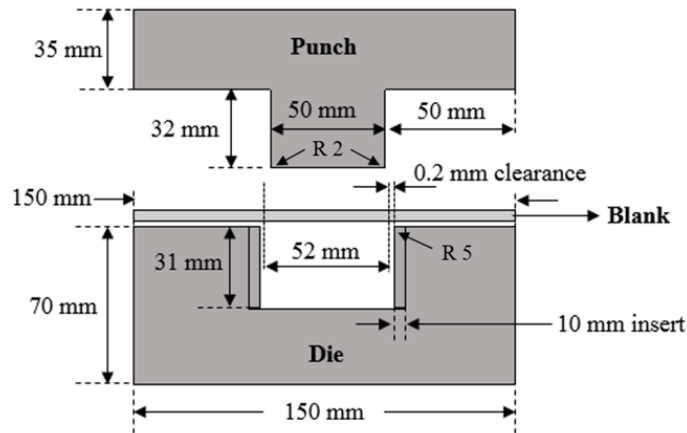


Figure 3. Schematic diagram of the actual design of the punch, die and blank.

A hat-shaped part was formed using the experimental tool displayed in Figure 3. The punch had a width of 50 mm and a punch profile radius of 2 mm. The die clearance required for punching mild steel was calculated using the following formula:

$$\text{Clearance, } C = 20\% \times t \tag{1}$$

For 1 mm,
 $1 \text{ mm} \times 0.2 = 0.2 \text{ mm}$

From the above calculation, the clearance between the punch and the die was 0.2 mm per side. The hat-shaped part was drawn over the radius at a constant velocity of 40 mm/s and the final punch displacement was limited to 29.2 mm. The blank holder was not used in this process. There was no use of lubrication or other mediums throughout the experiments. After the bending and removal of the final parts, measurements were taken for the springback reduction analysis.

Table 2. Parameters of the U-bending process [15].

Parameters	Values (unit)
Press holding time, P_t	1, 3, 5 (seconds)
Punch force, F_p	300 (kN)
Punch speed, S_p	10 (mm/s)

Specimen

The hat-shaped specimen was determined based on the results of previous studies [16]. The material selected for the hat-shaped specimen was mild steel (JIS G3131 SPHC) [17] as shown in Table 2. These steel sheets were chosen since they are commonly used in the car beam industry. In this experiment, 36 specimens with a rectangular length of 150 mm and a thickness of 1 mm were prepared. The blank width, b , was varied by 20 mm, 25 mm, and 30 mm for each of the experiment parameters, P1, P2, P3, and P0.

Table 3. The material properties of mild steel (JIS G3131 SPHC)[17].

Properties (Units)	Values
E-modulus (GPa)	210
Yield Stress (MPa)	263
Ultimate Tensile Strength (MPa)	355
Elongation (%)	42

Tooling

The designed punch has the following size dimensions of 150 mm width, 150 mm of length, 32 mm of an extruded channel with a 2 mm radius corner. On the other hand, the designed die has a width of 150 mm, a height of 70 mm, and length of 150 mm, with a 5 mm radius corner feature. These tools were specifically designed for the experiment based on previous studies [16-17]. Eight blocks with size dimensions of 10 mm (width), 50 mm (height), and 150mm (length) were prepared for the die insert. Next, each of the blocks underwent a milling process performed on a CNC milling machine

(Makino, KE55) using a custom-made radius tool of 10 mm to create a radius corner with a radius size of 10 mm. The blocks were then patterned along the corner radius as shown in Table 1. The insert corner shoulder was patterned using the Electrical Discharge Machining (EDM) die sinking operation (Mitsubishi, EA12D). Each insert of the die has two threaded holes for the screws to be clamped with the body of the die. The inserts used in this study for DSPM are shown in Figure 2.

The newly designed U-bending tool is depicted in Figure 3. The tool was made using the Electrical Discharge Machining (EDM) wire cut by SODICK VZ 300L. The material used for tooling was AISI H13, a tool steel material that is commonly used in the manufacturing industry due to its extremely high level of toughness and ductility vital characteristics when forming the product. Table 3 shows the chemical compositions of AISI H13. The AISI H13 steel has high toughness and hardenability. Telasang (2015) stated that AISI H13 has high dimensional stability and thermal fatigue resistance and was thus deemed as a suitable material for die casting tools [20].

Table 4. The chemical compositions of AISI H13.

Element	C	Mn	Si	Cr	Mo	V	P	S	Fe
wt%	0.36	0.38	0.90	4.82	1.19	0.86	0.017	0.004	Bal.

Springback Measurements

A standard 3D bridge Coordinate Measuring Machine (Tesastar-m, Swiss) was used to measure all the angles and distances of the hat-shaped parts in degrees and millimetres by sensing discrete points on the external surface of the blank with a circle probe as shown in Figure 4(a). This machine is commonly used due to its capability of measuring complex surfaces precisely [19-21]. The probe moves in three axes to make the measurement process more accessible, and the axe sensors monitor the position of the probe with micrometre precision. Furthermore, the measured location point was calculated and displayed using the dimensional measurement interface specification (PC-DMIS) software. The typical ratios of accuracy were between 1:3 to 1:20 and were considered to be accurate values for precision measurement. The measurement process begins with each set of three hat-shaped parts placed on top of the steel sheets and stacked to ensure that they were static and remained in a flat position during the measurements as shown in Figure 4(b).

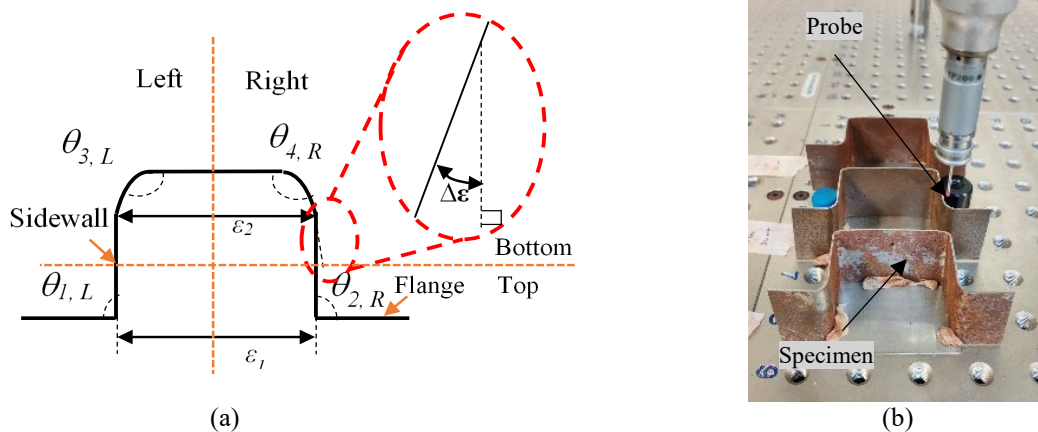


Figure 4. (a) Schematic diagram of the measured points and (b) 3D bridge CMM setup.

EXPERIMENTAL RESULTS

The data obtained in this study were analysed using two methods, namely the three-way analyses of variance (ANOVA) with replication and linear graphical analysis. These analyses were performed using the Microsoft Excel 2016 data analysis tools. The ANOVA analysis is commonly employed in springback prediction studies. For instance, Chen and Lee used ANOVA to investigate whether selected factors affected springback behaviour [22-23]. The authors successfully performed the experiment using ANOVA analysis to measure and validate the springback performance for each factor investigated. On the other hand, the graphical analysis was employed to study the effect of DSPM and press holding time on the impact of springback.

The study data were divided into three regions: (a) flange-wall region, (b) wall-bottom region, and (c) inner distance. The flange-wall region is the angle measurement from the flange to the sidewall on the left side ($\theta_{1,L}$) and right side ($\theta_{2,R}$), whereas the wall-bottom region is the angle measurement from the sidewall to the bottom on the left side ($\theta_{3,L}$) and right side ($\theta_{4,R}$). On the other hand, the inner distance is the distance measurement of the inner sidewall from the left inner sidewall to the right inner sidewall on the top (ϵ_1) and bottom (ϵ_2). The overall locations of each region consisting of six-point regions ($\theta_{1,L}$, $\theta_{2,R}$, $\theta_{3,L}$, $\theta_{4,R}$, ϵ_1 , and ϵ_2) were successfully expressed and tabulated (refer to appendices).

Three-Way ANOVA with Replication

For the three-way ANOVA analysis, three hypotheses consisting of hypothesis 1 (H1), hypothesis 2 (H2), and hypothesis 3 (H3) were proposed and applied to all three-region cases.

H1: The mean values of the measurement variable are equal for different values of the non-DSPM. (2)

H2: The mean values of the measurement variable are equal for different values of the DSPM. (3)

H3: The mean values of the measurement variable are equal for different values of the blank width, *b*. (4)

For H1 and H2, the F-value to FCrit-value (F critical) was compared and these hypotheses were rejected when $F > FCrit$, thus indicating that the mean values of the springback angle were not equal for different values of the DSPM and vice versa. On the other hand, the H3 hypothesis was rejected when $F > FCrit$, thus indicating an interaction between DSPM and press holding time in the springback effect. The P-value of ANOVA produced an alpha value of 0.9 that was used for comparison. When the P-value obtained is smaller than 0.9, the hypothesis is rejected. The results of both cases were analysed and discussed in the following section.

Case 1: Flange-wall region of $\theta_{1,L}$

For Case 1, the comparison of F-value to F-critical value as well as P-value to alpha value 1 for the flange-wall region of $\theta_{1,L}$ are shown in Table 5. The F-value of non-DSPM was higher than FCrit. These findings indicate that the non-DSPM was an impractical model to investigate the springback effect as no effect was observed between the die shoulder since there was no patterning. However, the P-value of non-DSPM was larger than 0.9 due to higher plastic occurrence after removing the parts from the jigs.

On the other hand, the F-value of DSPM was indicated by other prominent factors since it was smaller than the F-crit value. Therefore, the H1 for DSPM was not rejected. This observation was also supported as the P-value was higher than the alpha value of 0.9. Therefore, DSPM had a significant influence on the springback effect for the flange-wall region at $\theta_{1,L}$. In contrast, the F-value was higher than F-critical value for the source of variation for blank width, *b* and thus, H2 was rejected. This indicates that the factors for blank widths, *b*, does not significantly affect springback. Lastly, the values shown in Table 5 indicate that there was an interaction between DSPM and press holding time in the springback effect.

Table 5. Results of the three-way ANOVA for the flange-wall region of $\theta_{1,L}$.

Source of Variation	SS	df	MS	F	P-value	F-crit
Non-DSPM	9597.817	4	2399.454	140.3848	9.23E-07	4.120312
DSPM	0.876949	2	0.438474	0.065847	0.936443	3.402826
<i>b</i>	29447.42	3	9815.807	1474.063	2.46E-27	3.008787
Interaction	1.497391	6	0.249565	0.037478	0.99973	2.508189
Within	159.8164	24	6.659016			
Total	39207.427	39				

Case 2: Bottom-wall region of $\theta_{3,L}$

For Case 2, the comparison of F-value to F-crit value as well as P-value to alpha value 0.9 for the bottom-wall region of $\theta_{3,L}$ are shown in Table 6. The bottom-wall region of $\theta_{3,L}$ was analysed using three-way ANOVA with replication of three samples. For non-DSPM, it was observed that the F-value was bigger than the F-crit value. Additionally, the P-value was also higher than 0.9 and hence, H1 was rejected. These findings indicate that H1 was not acceptable for springback integrity in the bottom-wall region.

On the other hand, the F-value for DSPM in the bottom-wall region was lesser than the F-crit value. Thus, H1 was accepted. For the blank width, *b*, the F-value was higher than the F-crit value, and the P-value obtained was much higher than 0.9. Thus, H2 was rejected. These results indicate that the blank widths of 20 mm, 25 mm, and 30 mm did not significantly affect springback. For the Interaction values, the F-value was smaller than the F-crit value, and the P-value was higher than 0.05. Hence, the H2 hypothesis was rejected. Therefore, no interaction was observed between DSPM and press holding time in the springback effect for Case 2 as shown in Table 6.

Table 6. Results of the three-way ANOVA for the bottom-wall region of $\theta_{3,L}$.

Source of Variation	SS	df	MS	F	P-value	F-crit
Non-DSPM	8942.563	4	2235.641	278.7164	8.59E-08	4.120312
DSPM	1.245265	2	0.622632	0.096968	0.907938867	3.4028
<i>b</i>	27518.69	3	9172.896	1428.574	3.57499E-27	3.0088
Interaction	1.395289	6	0.232548	0.036217	0.999755814	2.5082
Within	154.1043	24	6.421014			
Total	36617.993	39				

Case 3: Inner-distance region of ϵ_1

For Case 3, the comparison of F-value to F-crit value as well as P-value to alpha value 0.9 for the inner-distance region of ϵ_1 are shown in Table 7. For non-DSPM, the F-value was higher than F-crit and therefore, H1 was not applicable for the springback effect at the inner-distance region.

For “DSPM”, the F-value was smaller than the F-crit value. Thus, the P-value was higher than 0.09, and H1 was not rejected. This result indicated that DSPM had a substantial influence on the springback effect for the inner-distance region of ϵ_l . For the blank width, b , the F-value was higher than the F-crit value. Likewise, the P-value obtained was higher than 0.9 and thus, H2 was rejected. For the “Interaction” values, the F-value was much lower than the F-crit value. Since the P-value was greater than 0.9, H2 was accepted and no interaction was observed between DSPM and press holding time in springback behaviour.

Table 7. Results of the three-way ANOVA for the inner-distance region of ϵ_l .

Source of Variation	SS	df	MS	F	P-value	F-crit
Non-DSPM	1366.769	4	341.6923	46.92682	3.85E-05	4.120312
DSPM	0.399973	2	0.199987	0.031526	0.969006	3.402826
b	4201.942	3	1400.647	220.7961	1.32E-17	3.008787
Interaction	0.211773	6	0.035295	0.005564	0.999999	2.508189
Within	152.2469	24	6.343622			
Total	7139.773	51				

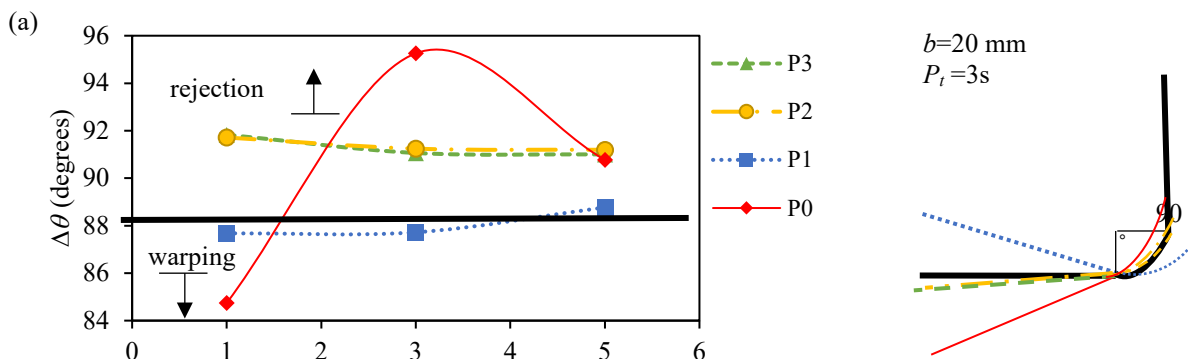
The ANOVA results are shown in Table 8. In conclusion, the hypotheses that were accepted for all three cases were H1 and H3. Therefore, DSPM has a substantial influence on the springback effect and there is no interaction between DSPM and press holding time in the springback effect. In contrast, the H2 hypothesis was rejected in all three cases, in which the factors of blank width, b , did not affect springback limitations for DSPM.

Table 8. Summary of ANOVA

Null Hypotheses	Comparison of F-value to F_{Crit} -value	Comparison of P-value to 0.05	Status
Case 1: Flange-wall region			
H1: non-DSPM	$F > F_{Crit}$	Larger	Reject
H2: DSPM	$F < F_{Crit}$	Smaller	Do not reject
H3: b	$F > F_{Crit}$	Larger	Reject
Case 2: Bottom-wall region			
H1: non-DSPM	$F > F_{Crit}$	Larger	Reject
H2: DSPM	$F < F_{Crit}$	Smaller	Do not reject
H3: b	$F > F_{Crit}$	Larger	Reject
Case 3: Inner distance-wall region			
H1: non-DSPM	$F > F_{Crit}$	Larger	Reject
H2: DSPM	$F < F_{Crit}$	Smaller	Do not reject
H3: b	$F > F_{Crit}$	Larger	Reject

Graphical Analysis

For the graphical analysis, Microsoft Excel 2016 was employed to generate a linear graphical analysis of 48 hat-shaped parts to investigate the reliability of the hat-shaped parts from the results obtained from the three-way ANOVA. Correspondingly, four linear graphs are discussed in this study. The graph and schematic diagram shown in Figure 6 to Figure 8 illustrate the springback angle acquired after unloading from the fixtures at selected press holding time intervals and blank width diameters. These diagrams depict the relationship between the total springback angle ($\Delta\theta$) and its components: $\Delta\theta_{l, L}$ (sidewall curl springback at the flange-wall), $\Delta\theta_{b, L}$ (sidewall curl springback at the bottom-wall), and $\Delta\epsilon_l$ opening curl springback at the inner-wall distance of the hat-shaped part). It was assumed that the optimum angle springback for the flange-wall and bottom-wall regions were 90 degrees and 50 mm as the optimum distance for the inner distance region of the hat-shaped parts. The straight line in the middle of the graph indicated the optimum line for the springback value of the obtained values after press forming of the hat-shaped parts. Hence, the pattern used was considered to be optimised if the value was close to the line.



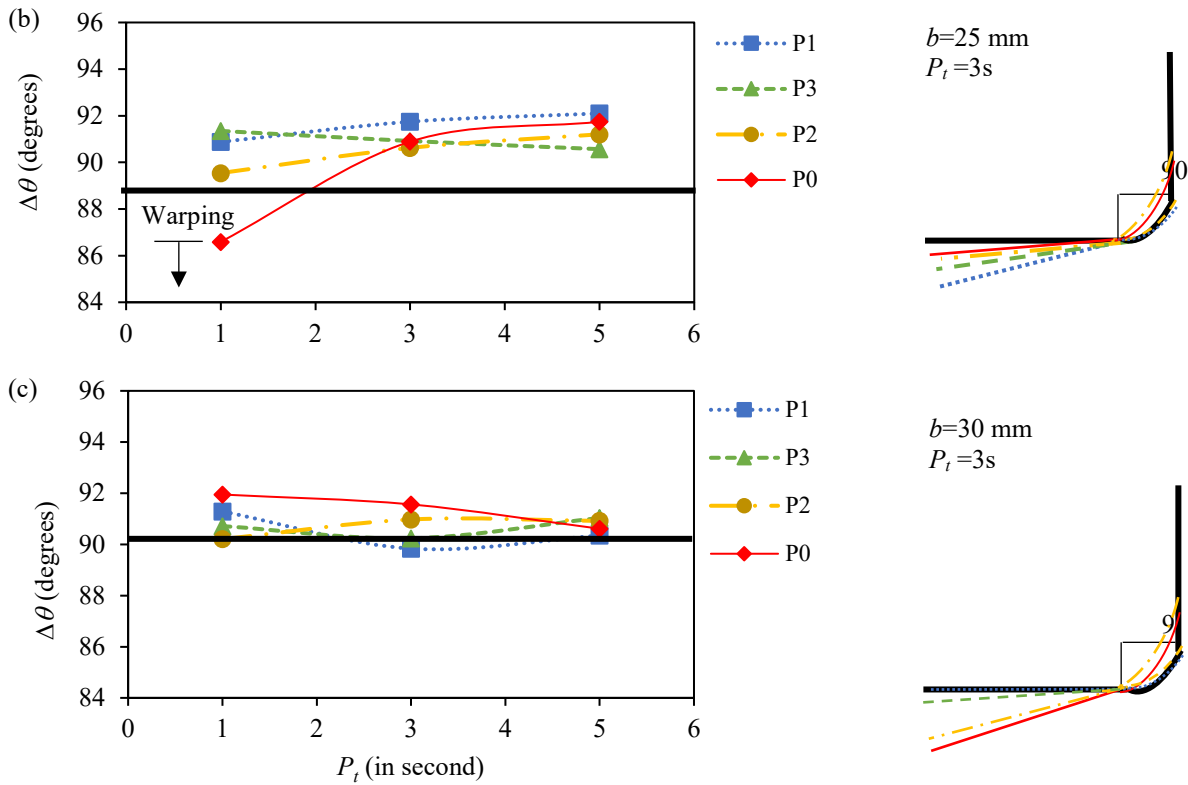


Figure 6. The graph of DSPM versus press holding time (P_t) at the left flange-wall region ($\theta_{l, L}$).

Relationship between DSPM versus P_t at the flange-wall of $\theta_{l, L}$

Figure 6 depicts the relationship between four different DSPM models with different press holding time intervals at the top flange-wall of the hat-shaped parts and their respective schematic diagrams. Figure 6(a) showed that the obtained angles of $\theta_{l, L}$ for P2 and P3 were close to the optimum line throughout the three selected press holding time intervals. On the other hand, the P0 or non-DSPM for the 20 mm blank width was further apart from the optimum line during the press holding time of 1 second and 3 seconds. One of the contributing factors for this observation was that there was no die patterning involved. Thus, the P0 was rejected as it did not have enough contact area, especially for the flange-wall regions during the 1-second and 3-seconds press holding time intervals to produce the optimal angles. However, the P0 during the 5-second press holding time was back to normal as the press holding time was longer despite being exposed to the sidewall warping. Sidewall warping is known as one of the major failures in sheet metal forming [26]. The surface contact area of the hat-shaped parts is given in Eq. (5) and Eq. (6).

$$\text{The surface contact area of the hat-shaped part} = \text{The surface area of DSPM} - \text{Surface area of the hat-shaped part}$$

$$\text{Sum of the surface contact area of the hat-shaped part} = \text{Sum of the surface area of DSPM} - \text{Sum of the surface area of the hat-shaped part}$$

$$A = (2\pi rh + \pi r^2) - (2\pi rh + \pi r^2) \times \text{Rib slots} \tag{5}$$

$$\Sigma A = \Sigma [(2\pi rh + \pi r^2)] - \Sigma [(2\pi rh + \pi r^2) \times \text{Rib slots}] \tag{6}$$

The formulas above were generated based on the surface area of the curved surface formula, $2\pi rh + \pi r^2$. Both formulas were multiplied by the number of the rib slots that touched the surface of the blank.

The flange-wall springback angle for P2 using a 25 mm blank width with 0.2 vertical pitch distance patterned at 3 seconds of P_t had the highest close rate to the optimal line compared to P1 and P3 as in Figure 6(b). However, the P0 or non-DSPM was closer to the optimal line than P1 but experienced warping at a P_t of 1 second. On the other hand, P1 using a 30 mm blank width was more optimal than P0 and P2 as shown in Figure 6(c). Hence, the nearest angles of DSPM to the optimal line at the flange-wall region on the top-left angle were P1, P2, and P3 but the farthest was P0 or non-DSPM. These results indicate that DSPM reduces the springback effect for press forming of hat-shaped parts.

Relationship between DSPM versus P_t at the bottom-wall of $\theta_{b, L}$

The relationship between four different DSPM models with different press holding time intervals at the left bottom-wall of the hat-shaped parts and its schematic diagram is shown in Figure 7. In Figure 7(a), P0 was found to have a large springback angle while the other DSPM patterns were similar to each other. P0 was found to have warping at the bottom-

wall of the hat-shaped parts. On the other hand, P1 and P2 were closer to the optimal angle as compared to other DSPM models. As shown in Figure 7(b), P1 was closer to the optimal angle as compared to P0.

In the bottom-wall region, P3 had more springback angle as compared to the other patterns since it had the lowest angle value from 90 degrees for both the blank width diameters of 25 mm and 30 mm as shown in Figures 7(b) and 7(c). In contrast, P1 had a lower springback angle between the other patterns since it had the nearest angle value to 90 degrees for both blank width diameters of 25 mm and 30 mm as shown in Figures 7(b) and 7(c). Therefore, P0 had the furthest deviation from the original shape of the hat-shaped parts for the bottom-wall region of θ_3, L . In the bottom-wall region, both P1 and P2 showed the best pattern to reduce springback behavior.

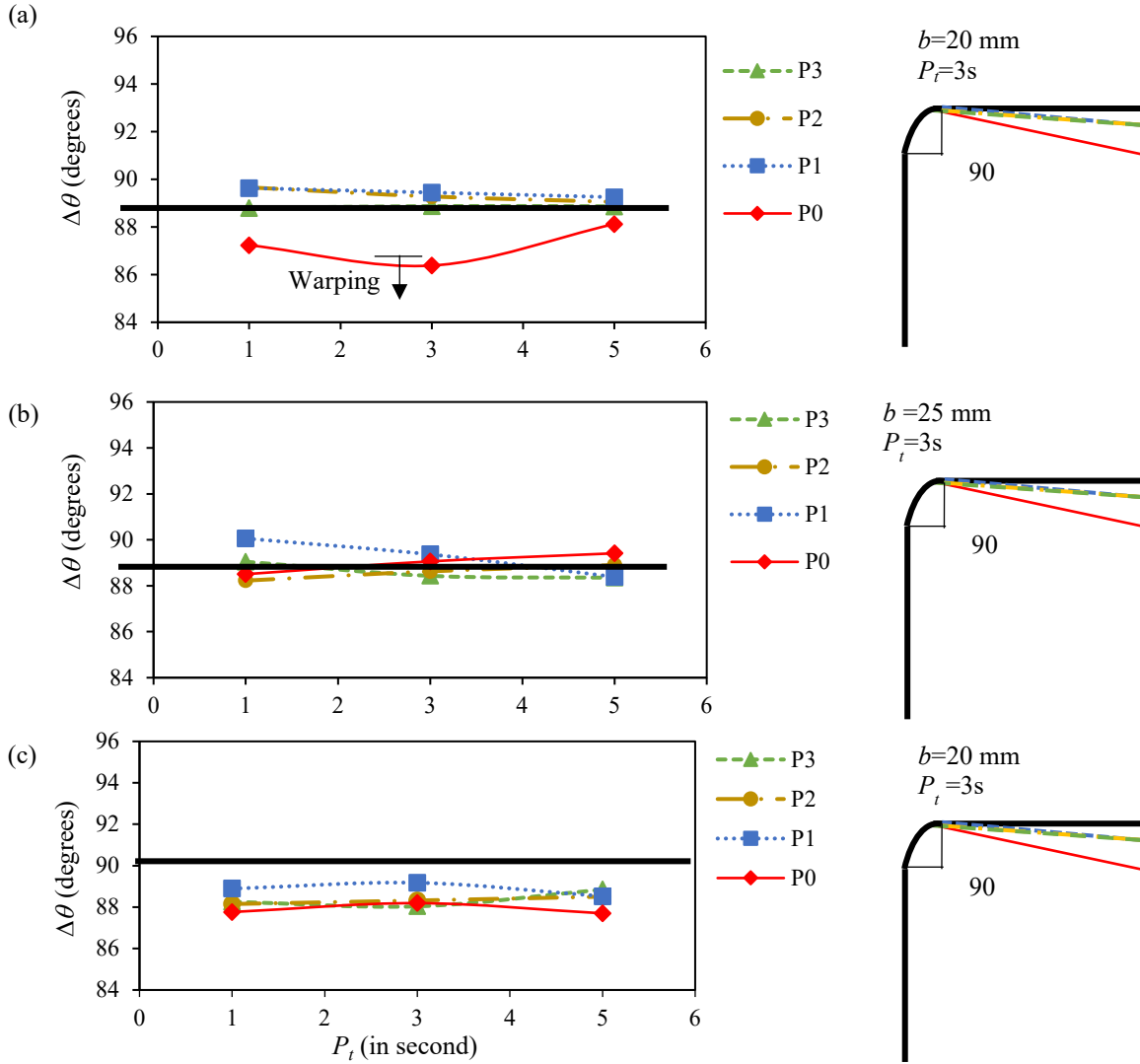


Figure 7. Graph of DSPM versus press holding time (P_t) at the left bottom-wall region (θ_3, L).

Relationship between DSPM versus P_t at the inner distance of ϵ_1

Figure 8 shows the relationship between four different DSPM models with the press holding time intervals at the top inner-distance of the formed hat-shaped parts. For inner-distance regions, 50 mm was assumed as the optimum distance for the best hat-shaped parts. The optimum distance was chosen based on the size of the punch used. The ideal condition for a blank width of 20 mm was P3 at 1 second of the press holding time. However, as P_t increased, the distance value decreased, as shown in Figure 8(a). One of the reasons for this observation could be due to the increased sliding stress between the tool and the blank as P_t increased.

On the other hand, the same distance value was observed for every press holding time used while forming the hat-shaped part using P0 at a 20 mm blank width. This consistency may be due to the absence of patterns at the die shoulder on the inner-distance of the hat-shaped components, as indicated by the correlation observed from Figure 8(b) and 8(c), in which the same trends occurred in other regions of the P0 model. Additionally, the best condition for a 25 mm blank width was obtained at 5 seconds using P2 as shown in Figure 8(b). As expected, the hat-shaped parts using P0 were rejected in this condition due to inaccurate distance values that were more than 0.4% of the accepted value. In Figure 8(c), P2 achieved a precise distance at 1 second for a 30 mm bank width. Hence, P0 was rejected and P2 was the best model for improving the springback effect at the inner-distance region. In all scenarios studied in this experiment, the

DSPM models exhibited significant decreases in springback values except P0. In conclusion, the finished part's of these DSPM models able to improves it's dimensional accuracy.

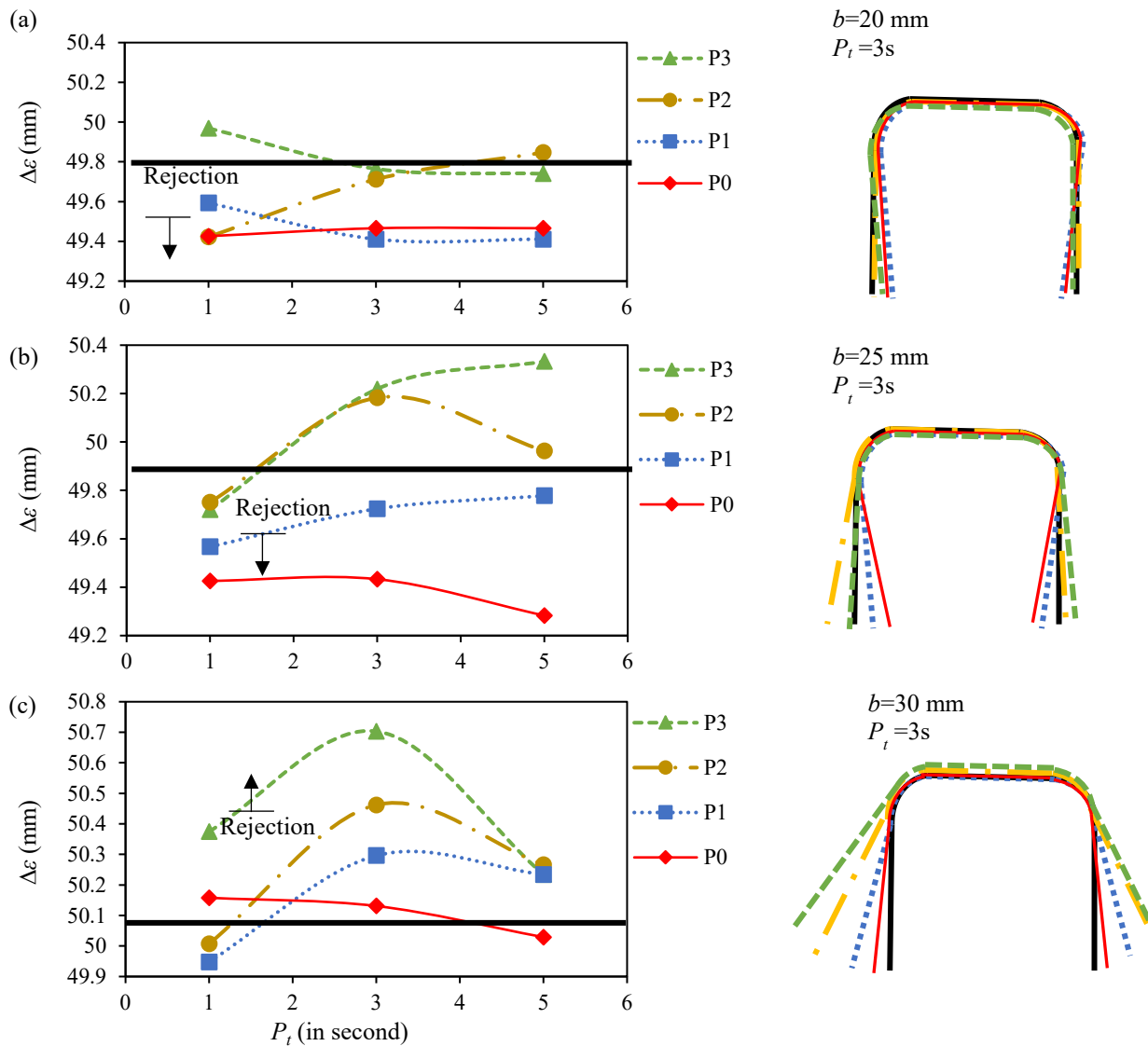


Figure 8. Graphical illustration of DSPM versus P_t at the inner-distance top, ϵ_I .

CONCLUSION

In conclusion, four novel DSPM models for U-bending of hat-shaped parts were proposed and assessed in this study to minimize the springback of the U-bending part. A blank shape optimization procedure using the three-way ANOVA method and graphical analysis is discussed. The experiment parameters studied include the type of DSPM (pattern 1, 2, 3 and non-pattern), blank width (20 mm, 25 mm, and 30 mm), and press holding time (1s, 3s, and 5s). To sum up, the longer the press holding time, the lesser the springback angle as the sliding stress between blank and die wall is reduced. Pattern 2 with a radius of 5 mm and rib size of 0.4 mm successfully minimized springback by increasing the contact area and reducing sliding stress between the die shoulder and surface of the blank. Because the flow of material is slightly analysed in this investigation, the blank width, b , has a small impact on springback behaviour of U-bending hat-shaped. For future research, mathematical modeling to describe the material behavior of any grain size in each DSPM hat-shaped parts shall be considered to enhance further the springback of U-bending.

ACKNOWLEDGEMENT

The authors would like to thank UMP for funding this work under an internal grant RDU182203-4.

REFERENCES

[1] C. Qi *et al.*, "On design of hybrid material double-hat thin-walled beams under lateral impact," *Int. J. Mech. Sci.*, vol. 118, pp. 21–35, Nov. 2016, doi: 10.1016/j.ijmecsci.2016.09.009.

- [2] C. Qi, Y. Sun, and S. Yang, "A comparative study on empty and foam-filled hybrid material double-hat beams under lateral impact," *Thin-Walled Struct.*, vol. 129, pp. 327–341, Aug. 2018, doi: 10.1016/j.tws.2018.04.018.
- [3] C. Mertin and G. Hirt, "Numerical and experimental investigations on the springback behaviour of stamping and bending parts," *Procedia Eng.*, vol. 207, pp. 1635–1640, Jan. 2017, doi: 10.1016/J.PROENG.2017.10.1091.
- [4] D. K. Leu and Z. W. Zhuang, "Springback prediction of the vee bending process for high-strength steel sheets," *J. Mech. Sci. Technol.*, vol. 30, no. 3, pp. 1077–1084, Mar. 2016, doi: 10.1007/s12206-016-0212-8.
- [5] J. Agirre, L. Galdos, E. Saenz de Argandoña, and J. Mendiguren, "Hardening prediction of diverse materials using the Digital Image Correlation technique," *Mech. Mater.*, vol. 124, pp. 71–79, Sep. 2018, doi: 10.1016/j.mechmat.2018.05.007.
- [6] M. H. Parsa, S. Nasher al ahkami, H. Pishbin, and M. Kazemi, "Investigating spring back phenomena in double curved sheet metals forming," *Mater. Des.*, vol. 41, pp. 326–337, Oct. 2012, doi: 10.1016/j.matdes.2012.05.009.
- [7] W. D. Carden, L. M. Geng, D. K. Matlock, and R. H. Wagoner, "Measurement of springback," *Int. J. Mech. Sci.*, vol. 44, no. 1, pp. 79–101, Jan. 2002, doi: 10.1016/S0020-7403(01)00082-0.
- [8] A. Bardelcik *et al.*, "Effect of cooling rate on the high strain rate properties of boron steel," *Int. J. Impact Eng.*, 2010, doi: 10.1016/j.ijimpeng.2009.05.009.
- [9] V. Paunoiu, V. Teodor, N. Baroiu, and C. Maier, "A contribution to multi-channel sheet hydroforming," *Procedia Manuf.*, vol. 29, pp. 248–255, 2019, doi: 10.1016/j.promfg.2019.02.133.
- [10] U. Pettersson and S. Jacobson, "Textured surfaces for improved lubrication at high pressure and low sliding speed of roller/piston in hydraulic motors," *Tribol. Int.*, vol. 40, no. 2 SPEC. ISS., pp. 355–359, Feb. 2007, doi: 10.1016/j.triboint.2005.11.024.
- [11] L. De Chiffre, H. Kunzmann, G. N. Peggs, and D. A. Lucca, "Surfaces in precision engineering, microengineering and nanotechnology," *CIRP Ann. - Manuf. Technol.*, vol. 52, no. 2, pp. 561–577, Jan. 2003, doi: 10.1016/S0007-8506(07)60204-2.
- [12] A. A. G. Bruzzone, H. L. Costa, P. M. Lonardo, and D. A. Lucca, "Advances in engineered surfaces for functional performance," *CIRP Ann. - Manuf. Technol.*, vol. 57, no. 2, pp. 750–769, Jan. 2008, doi: 10.1016/j.cirp.2008.09.003.
- [13] A. Godi *et al.*, "Testing of newly developed functional surfaces under pure sliding conditions," *Tribol. Lett.*, vol. 51, no. 1, pp. 171–180, Jul. 2013, doi: 10.1007/s11249-013-0162-6.
- [14] R. Bahloul, S. Ben-Elechi, and A. Potiron, "Optimisation of springback predicted by experimental and numerical approach by using response surface methodology," *J. Mater. Process. Technol.*, 2006, doi: 10.1016/j.jmatprotec.2005.11.009.
- [15] M. Mobin, M. Basik, and J. Aslam, "Pineapple stem extract (Bromelain) as an environmental friendly novel corrosion inhibitor for low carbon steel in 1M HCl," *Measurement*, vol. 134, pp. 595–605, Feb. 2019, doi: 10.1016/J.MEASUREMENT.2018.11.003.
- [16] K. Sato, T. Inazumi, A. Yoshitake, and S.-D. Liu, "Effect of material properties of advanced high strength steels on bending crash performance of hat-shaped structure," *Int. J. Impact Eng.*, vol. 54, pp. 1–10, Apr. 2013, doi: 10.1016/J.IJIMPENG.2012.10.012.
- [17] J. Choung, "Micromechanical damage modeling and simulation of punch test," *Ocean Eng.*, vol. 36, no. 15–16, pp. 1158–1163, 2009, doi: 10.1016/j.oceaneng.2009.08.004.
- [18] M. F. Zamri and A. R. Yusoff, "Heuristic design of U-shaped die cooling channel for producing ultra-high strength steel using hot press forming," *Int. J. Adv. Manuf. Technol.*, vol. 97, no. 9–12, pp. 4101–4114, Aug. 2018, doi: 10.1007/s00170-018-2097-4.
- [19] Y. Abe, S. Watanabe, Z. Hamedon, and K. Mori, "Prevention of wrinkling in shrink flanging of ultra-high strength steel sheets using gradually contacting punch," *J. Japan Soc. Technol. Plast.*, vol. 55, no. 639, pp. 341–345, 2014, doi: 10.9773/sosci.55.341.
- [20] M. Åsberg *et al.*, "Influence of post treatment on microstructure, porosity and mechanical properties of additive manufactured H13 tool steel," *Mater. Sci. Eng. A*, vol. 742, pp. 584–589, Jan. 2019, doi: 10.1016/J.MSEA.2018.08.046.
- [21] F. Shen and J. Tarbutton, "A voxel based automatic tool path planning approach using scanned data as the stock," in *Procedia Manufacturing*, 2019, vol. 34, pp. 26–32, doi: 10.1016/j.promfg.2019.06.110.
- [22] I. Ragai, D. Lazim, and J. A. Nemes, "Anisotropy and springback in draw-bending of stainless steel 410: experimental and numerical study," *J. Mater. Process. Technol.*, vol. 166, no. 1, pp. 116–127, 2005, doi: 10.1016/j.jmatprotec.2004.08.007.
- [23] İ. Karaağaç, "The evaluation of process parameters on springback in V-bending using the flexforming process," *Mater. Res.*, vol. 20, no. 5, pp. 1291–1299, 2017, doi: 10.1590/1980-5373-MR-2016-0799.
- [24] S. . Lee and D. . Yang, "An assessment of numerical parameters influencing springback in explicit finite element analysis of sheet metal forming process," *J. Mater. Process. Technol.*, vol. 80, pp. 60–67, 1998, doi: 10.1016/S0924-0136(98)00177-0.
- [25] P. Chen and M. Koç, "Simulation of springback variation in forming of advanced high strength steels," *J. Mater. Process. Technol.*, vol. 190, no. 1, pp. 189–198, 2007, doi: 10.1016/j.jmatprotec.2007.02.046.
- [26] D. Y. Yang *et al.*, "Flexibility in metal forming," *CIRP Ann.*, vol. 67, no. 2, pp. 743–765, Jan. 2018, doi: 10.1016/J.CIRP.2018.05.004.